Using rock physics to improve Q_p quantification in seismic data

Yi Shen and Jack Dvorkin

ABSTRACT

We derived an approximate closed-form solution relating V_p to Q_p using rock physics modeling. This solution is validated using well data in which the elastic properties were measured and Q was derived numerically using rock physics. We applied our new $Q_p - V_p$ equation to synthetic seismic data, which produced an improved Q model.

INTRODUCTION

Gas pockets or clouds are notoriously challenging problems for reservoir identification and interpretation (Billette and Brandsberg-Dahl, 2005), because strong attenuation and low-velocity anomalies are present in them. Attenuation degrades the seismic image quality by decaying the image amplitude, lowering the image resolution, distorting the phase of events, and dispersing the velocity. Low-velocity mispositions and distorts the events. These problems impede accurate image interpretation for hydrocarbon production and well positioning.

To mitigate the effects of gas accumulations on the image, we need a better understanding of the properties of the gas used for imaging the subsurface. Compressional velocity (V_p) and compressional Q (Q_p) play an important role in compensating for the gas-induced distortion in the image. However, an accurate estimation of these two properties is limited to the insufficient information from the acquired seismic data and to the ambiguity in the distorted effects of the images from these two parameters. A quantification of the relation between V_p and Q_p brings additional information to the seismic inversion for a better estimation of these two properties.

It has been observed from field data (He and Cai, 2012; Zhou et al., 2014) that high-compressional attenuation comes with low-compressional velocity in most situations. However, very few studies have analytically linked these two properties. Rock physics has built several models (Dvorkin et al., 2014; Muller et al., 2010) of V_p and Q_p based on rock properties (such as porosity, saturation and others), which may implicitly quantify the relation between these two parameters. But, these existing models for V_p and Q_p, based on rock physics properties, confine the measurements of these two parameters to a constrained area limited by the well locations. A model that provides an analytical relation between V_p and Q_p would allow us to approxi-

mately relate Q_p to V_p without going through direct rock physics modeling, which in turn would improve the accuracy of the seismic inversion of V_p and Q_p.

In this study, we first derived an approximate closed-form solution directly relating V_p to Q_p using rock physics modeling. Next, we validated this relation using field well data. Last, we applied our new $Q_p - V_p$ equation to synthetic seismic data, which produced an improved Q model.

THEORY

Modeling seismic attenuation

Seismic attenuation primarily occurs either at a gas reservoir or in the presence of shallow gas pockets. Wave-induced variations of pore pressure in the partially saturated rock results in oscillatory liquid flow. The viscous losses during this oscillatory liquid flow cause wave attenuation. The frequencies of the wave span broad frequencies and scales, which can be categorized as macroscopic, mesoscopic, and microscopic based on the spatial scale of the heterogenities. Mesoscopic flow, rather than macroscopic and microscopic flow, is engaged at the seismic exploration frequency range, and is considered to be the main mechanism for the fluid-related seismic attenuation.

Seismic attenuation, parameterized by quality factor Q, is a function of frequency. According to the standard linear solid model, we are able to obtain the relation between $1/Q$ and frequency, and therefore derive the maximum $1/Q$:

$$Q_{\max}^{-1} = \frac{M_\infty - M_0}{2\sqrt{M_\infty M_0}}, \tag{1}$$

where $Q_{\max}^{-1}$ is the maximum inverse quality factor, M_0 is the compressional modulus at very high frequency, and M_∞ is the compressional modulus at very low frequency. The compressional modulus is the product of the bulk density and P-wave velocity squared. This equation provides the upper bound for attenuation without addressing its frequency dependence. Therefore, we use $Q_{\max}^{-1}$ to describe the effects of seismic attenuation.

According to Dvorkin et al. (2014), in partially saturated rock, viscoelastic effects and attenuation may arise from the oscillatory liquid cross-flow between fully liquid-saturated patches and the surrounding rock with partial gas saturation. The reaction of rock with patchy saturation to loading by the elastic wave depends on the frequency. If it is low and the loading is slow, the oscillations of the pore pressure in a fully liquid-saturated patch and partially saturated domains next to it are equilibrating. The patch is "relaxed." Mavko et al. (1991) derived an approximation to Gassmann fluid substitution equation (Gassmann, 1951) for the compressional modulus of the partially saturated rock as follows:

$$M_0 = M_S \frac{\phi M_{Dry} - (1+\phi)K_F M_{Dry}/M_S + K_F}{(1-\phi)K_F + \phi M_S - K_F M_{Dry}/M_S}, \tag{2}$$

where M_S is the compressional modulus of the mineral phase, M_{Dry} is the compressional modulus of the dry frame of the rock, ϕ is the total porosity, and K_F is the effective bulk modulus of the fluid in the rock.

Conversely, if the frequency is high and the loading is fast, the resulting oscillatory variations of pore pressure cannot equilibrate between the fully saturated patch and the domain outside. The patch is "unrelaxed." For a high frequency, we can use the patchy saturation equation (Mavko et al., 1991), which expresses the unrelaxed compressional modulus as the harmonic average of the compressional moduli of the wet rock M_W and rock with only gas M_G:

$$\frac{1}{M_\infty} = \frac{S_W}{M_W} + \frac{1 - S_W}{M_G}, \tag{3}$$

where

$$M_W = M_S \frac{\phi M_{Dry} - (1+\phi) K_W M_{Dry}/M_S + K_W}{(1-\phi) K_W + \phi M_S - K_W M_{Dry}/M_S}, \tag{4}$$

$$M_G = M_S \frac{\phi M_{Dry} - (1+\phi) K_G M_{Dry}/M_S + K_G}{(1-\phi) K_G + \phi M_S - K_G M_{Dry}/M_S}, \tag{5}$$

K_W and K_G are the bulk modulus of water and gas, respectively, and S_W is water saturation.

Modeling velocity

The compressional velocity of rock is related to the compressional modulus M_0 and its bulk density ρ as

$$V_p = \sqrt{\frac{M_0}{\rho}}. \tag{6}$$

Linking seismic attenuation and velocity: closed-form solution

V_p and Q_p are functions of a number of rock properties: M_{Dry}, M_S, S_W, ϕ, K_W, K_G and ρ. Model building of V_p and Q_p based on these rock parameters is the intermediate step to link V_p with Q_p in our study. Because a change in these rock properties results in changes in V_p and Q_p to different degrees, we only linked V_p with Q_p using the rock properties which, when modified, generate a significant change in these two properties and therefore in their relation. We assigned a spatially constant value to the rest of the rock parameters. A prior knowledge of the lithology of the areas of our study and measurements from well data enabled us to obtain an average value to approximately quantify properties of little influence on V_p and Q_p. Figure 1 is the sensitivity curve showing the influence of a change in these rock properties on a change in V_p and Q_p. The variation of the rock properties are shown in Table 1.

The results show that a perturbation in M_{Dry} leads to the most significant change in both V_p and Q_p among these rock parameters. Therefore, we linked V_p with Q_p using M_{Dry} in our study.

Table 1: The variation of the rock properties for Figure 1

Rock properties	Minimum value	Maximum value	background value
K_W	0.9521	3.9305	2.4413
K_G	0.0088	0.0364	0.0226
M_S	37.6740	155.5260	96.6000
ρ	0.8853	3.6547	2.2700
M_{Dry}	3.9000	16.1000	10.0000
ϕ	0.1170	0.4830	0.3000
S_W	0.1170	0.4830	0.3000

The rock property M_{Dry} is not a direct measurable parameter from the well log. The previous studies (Raymer et al., 1980; Dvorkin and Nur, 1996) built the rock physics model to compute M_{Dry} using other parameters. However, these models have not provided an analytical equation conveniently used to derive the relation between V_p and Q_p. Based on the idea that as the rock becomes softer, its moduli decreases as pore space increases, and the porosity-induced change in rock moduli should be proportional to ϕ, we propose a new model in this study for M_{Dry} with a simple equation:

$$\frac{M_{Dry}}{M_S - M_{Dry}} = \frac{\alpha_{Dry}}{\phi}, \tag{7}$$

where α_{Dry} is a positive number. The large α_{Dry} slowly increases the porosity-induced change of the rock moduli as the porosity increases. As a result, the dry rock moduli with a larger α_{Dry} is larger than the one with a smaller α_{Dry} for a fixed ϕ, as shown in Figure 2(a).

Equation 7 shows that M_{Dry} depends on M_S and ϕ. By substituting Equation 7 into Equations 1 and 6 to eliminate M_{Dry}, we obtained new sensitivity curves in Figure 3 showing the amount of changes of V_p and Q_p caused by a perturbation in the rock properties M_S, S_W, ϕ, K_W, K_G and ρ. The results show that a perturbation in M_S and ϕ results in the most significant change in both V_p and Q_p among these rock parameters. Because M_S can be estimated if the mineral content of the reservoir rock is known, we mainly studied the effects of the variation of ϕ on V_p and Q_p.

The porosity ϕ is a measure of the fraction of open space in the rock. Pore space softens the rock and makes its moduli decrease, which makes the compressional velocity decrease as shown in the lower panel of Figure 2(b). Also, the oscillatory liquid cross-flow between the gas and fluid in the pore space causes attenuation, as shown in the top panel of Figure 2(b). We linked V_p and Q_p by way of ϕ. Substituting

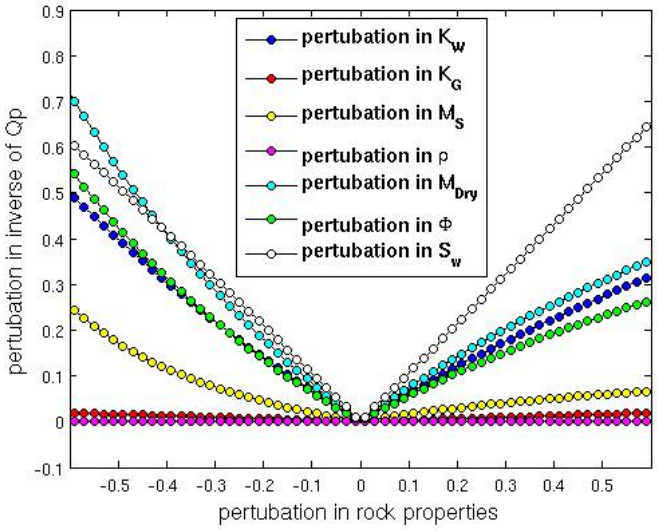

(a)

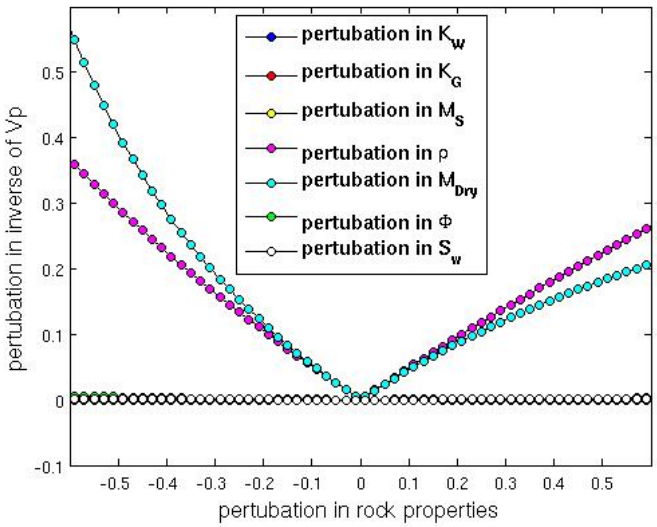

(b)

Figure 1: The sensitivity of (a) Q_p and (b) V_p to a change in the rock properties of M_{Dry}, M_S, S_W, ϕ, K_W, K_G, ρ. The background rock parameters are $K_W = 2.4413; K_G = 0.0226; M_S = 96.6; \rho = 2.27; M_{Dry} = 10; \phi = 0.3; S_W = 0.3$. [**NR**]

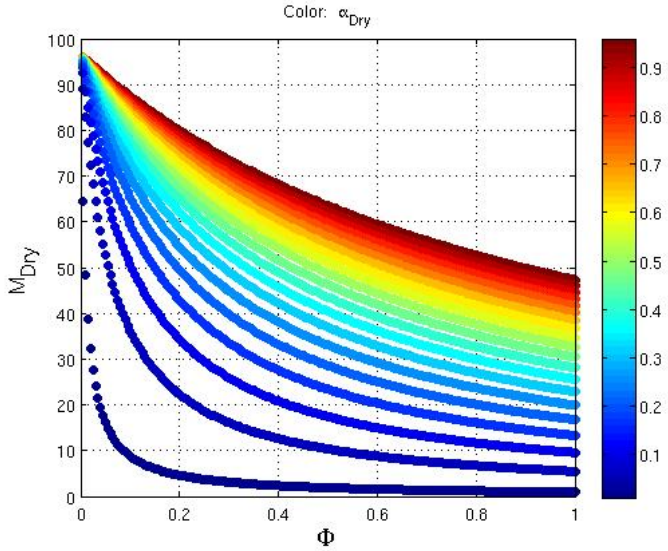

(a)

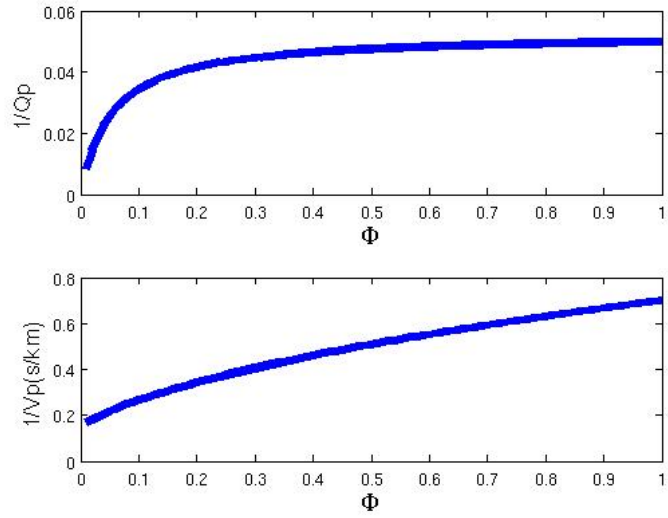

(b)

Figure 2: (a) Our new model for rock properties M_{Dry} as a function of ϕ and α_{Dry}, with $M_S = 96.6$ (b) The relations of ϕ with Q_p (top) and V_p (bottom), with $K_W = 2.4413; K_G = 0.0226; M_S = 96.6; \rho = 2.27; \alpha_{Dry} = 0.05; S_W = 0.3$. [**NR**]

ϕ with V_p, and assuming $M_\infty \approx M_0$ in the denominator of the right side of Equation 1, we were able to have the relation between V_p and Q_p

$$Q_p^{-1} = \frac{1}{2}\frac{c_1 V_p^{-2}}{c_2 V_p^{-2} + c_3} - \frac{1}{2}, \tag{8}$$

where

$$\begin{aligned} c_1 &= (\alpha_{Dry} + \alpha_W)(\alpha_{Dry} + \alpha_G), \\ c_2 &= S_W(\alpha_{Dry} + \alpha_F)(\alpha_{Dry} + \alpha_G) + (1 - S_W)(\alpha_{Dry} + \alpha_F)(\alpha_{Dry} + \alpha_W), \\ c_3 &= \frac{\rho}{M_S}(S_W(\alpha_{Dry} + \alpha_F)(\alpha_W - \alpha_G) + (\alpha_{Dry} + \alpha_W)(\alpha_G - \alpha_F)), \end{aligned} \tag{9}$$

and

$$\begin{aligned} \alpha_F &= \frac{K_F}{(M_S - K_F)}, \\ \alpha_G &= \frac{K_G}{(M_S - K_G)}, \\ \alpha_W &= \frac{K_W}{(M_S - K_W)}. \end{aligned} \tag{10}$$

Figure 4 shows the relations between $1/V_p$ and $1/Q_p$. The solid circles are the exact relation using Equations 1 and 6, and the nonfilled circles are calculated by the approximated Equation 8. These two curves have no large bias overall, and match very well for small porosity. From these results, we observe that the decrease of the compressional velocity corresponds to strong attenuation, in accordance with the observation from field data distorted by gas anomalies.

VALIDATING THE CLOSED-FORM SOLUTION USING WELL DATA

We use a field gas log to validate our theory. The black curve shown in Figures 5(a) through 5(g) are the rock properties measured from the log. We calculated the Q value using Equation 1 in Figure 5(h). The log has a low-water saturation at depths from 1.25 to 1.27 kilometers (km) and 1.31 to 1.32 km, indicating gas sand. We observe that both V_p and Q_p are small in the gas sand.

We first computed the dry-rock compressional moduli M_{1Dry} from the provided rock properties using the Gassmann-Mavko equation (Mavko et al., 1991). We then superimposed M_{Dry} using our new model on M_{1Dry} in Figure 6(a), finding a good match of our model with the gas sand shown in blue at $\alpha_{Dry} = 0.05$. Then, we computed the approximated Q_p for the gas sand using Equation 1, shown as the red curve in Figure 5(h), with the assumption that α_{Dry} is 0.05 for our M_{Dry} and that M_∞ equals to M_0 in the denominator of the right side of Equation 1.

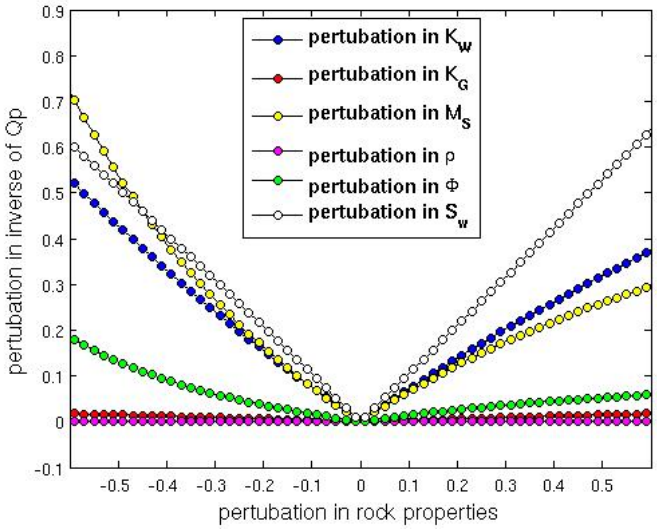

(a)

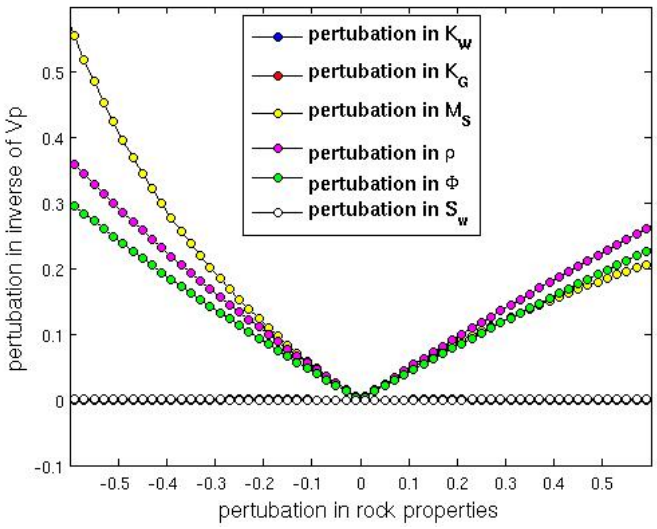

(b)

Figure 3: The amount of changes of (a)Q_p and (b)V_p caused by a perturbation in the rock properties M_S, S_W, ϕ, K_W, K_G, ρ. The unchanged rock parameters are $K_W = 2.4413; K_G = 0.0226; M_S = 96.6; \rho = 2.27; \alpha_{Dry} = 0.05; \phi = 0.3; S_W = 0.3$. [**NR**]

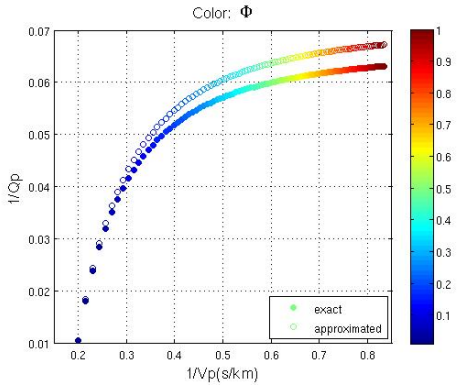

Figure 4: The relations between $1/V_p$ and $1/Q_p$, with $K_W = 2.4413; K_G = 0.0226, M_s = 96.6; \rho = 2.27$. [**NR**]

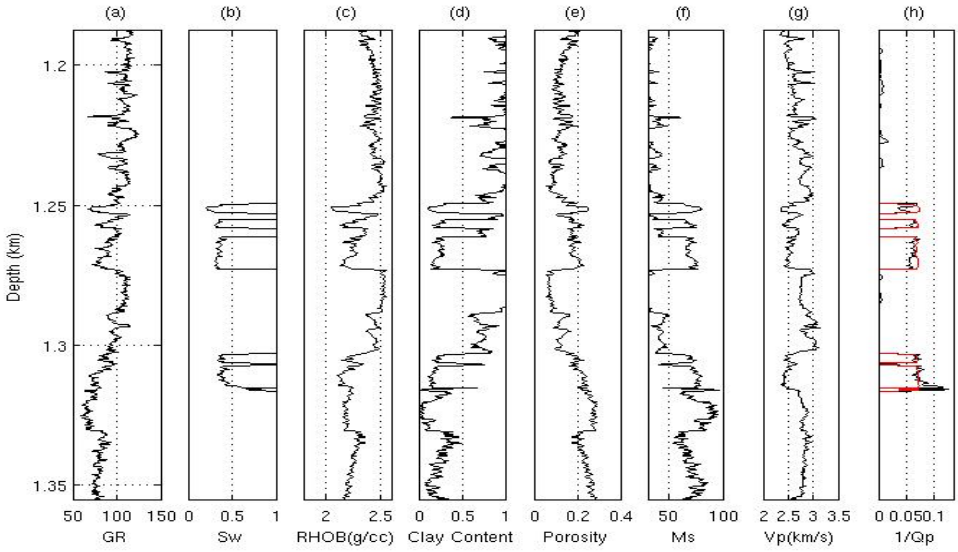

Figure 5: Well data used to verify our approximate relations. [**NR**]

Figure 6(b) shows the relation between V_p and Q_p. The blue dots are the log data in which the trend is approximated by red dots with a water saturation of $S_W = 0.37$. The approximated trend matches our predicted relation well by the black line using Equation 8. It slightly over-estimates direct computations because of our simplified new M_{Dry} model and our approximated equation (Equation 8).

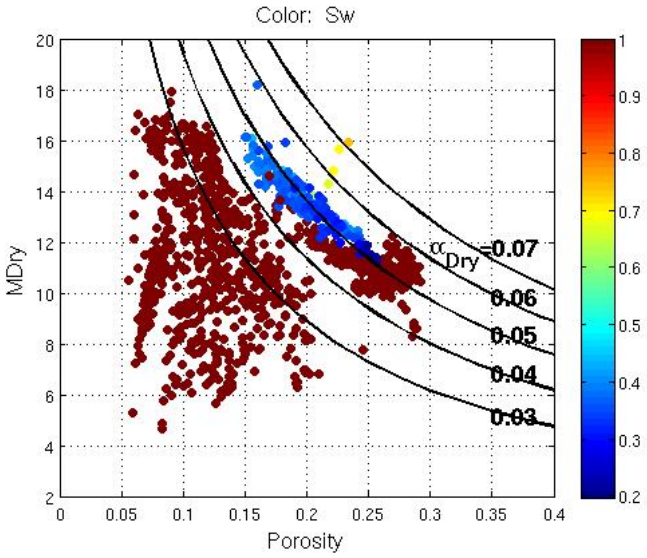

(a)

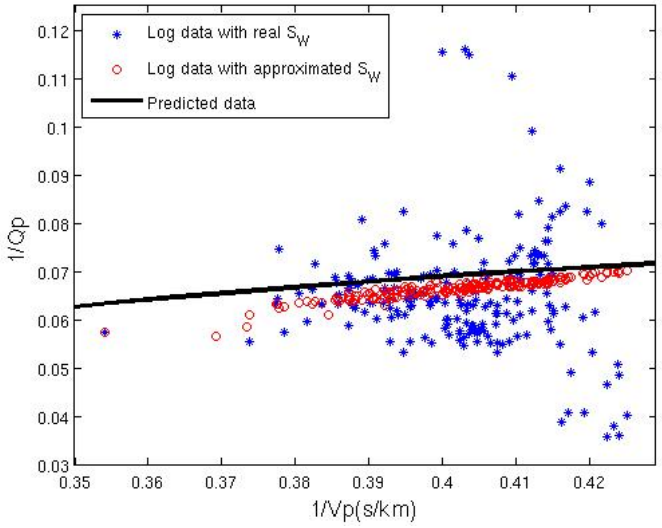

(b)

Figure 6: (a)The M_{Dry} model is superimposed on the log; (b)The relation between V_p and Q_p of the log. [**NR**]

SEISMIC APPLICATION

We forwarded model a synthetic seismic dataset using the V_p and Q_p models present in Li et al. (2015), as shown in Figure 7.Li et al. (2015) built the synthetic models based on the shallow unconsolidated sand reservoir model in Wang et al. (2013). A shallow gas pocket with 70% gas saturation is located in the upper part of the second layer, which has low velocity and high attenuation. Its rock properties porosity and gas saturation are shown in Figure 8. The shallow shale porosity in Figure 8 is arbitrarily assumed to be very small and unrelated to the velocity model. This assumption has no impact on our application in this study, because we do not use porosity in shale for our Q_p computations.

To synthesize the seismic data, we downward propagated and attenuated the wavefield (Shen et al., 2013, 2014) using the V_p and Q_p models in Figure 7 with 53 sources and 801 receivers uniformly distributed on the surface. A Ricker wavelet with 20 Hz central frequency was used as the source wavelet, and the density model was assumed to be spatial constant.

In practice, V_p and Q_p models are unknown in real fields. It is necessary to invert for these models that are important for generating a seismic migration image. The goal of our study is to invert for accurate Q_p models from the synthetic seismic data with the assumption that the correct V_p model is known. As a result, we were able to obtain a seismic migration image with a correction of its Q_p effects.

We inverted for the Q_p model shown in Figure 9(a) using wave-equation migration Q analysis (Shen et al., 2013, 2014), and used spatial constant $Q_p = 100,000$ as the initial model. The inverted Q_p model in Figure 9(a) highlights the area with high attenuation. However, the sparse reflectors and the limitation of this method result in a low resolution of the Q_p model, especially in the vertical direction. Therefore, we used the relation given by Equation 8 as a regularization term in the inversion workflow developed by Shen et al. (2013, 2014). In reference to the correct Q_p model in 7(b), the inverted Q_p model with regularization in Figure 9(b) has higher vertical resolution and a better shape than the one in Figure 9(a).

Figure 10(a) is the migration image without knowing the correct Q_p model for the gas sand. The events under the gas sand are attenuated, in terms of their dimming amplitude, stretching and distorted wavelets in Figure 10(a). Figure 10(b) is the migration image compensated using the inverted Q_p model in Figure 9(b). The results show that compensation adequately restores both the amplitude and frequency of the events below the gas sand.

CONCLUSION

We derived an approximate closed-form solution relating V_p to Q_p using rock physics modeling. This solution is validated using well data in which the elastic properties were measured and Q was derived numerically using rock physics. Finally we applied

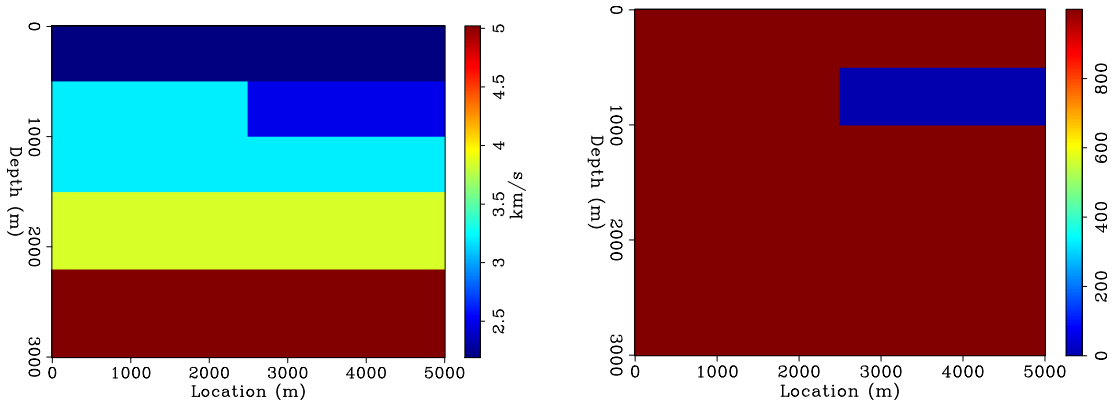

(a) (b)

Figure 7: (a) Correct V_p model (b) Correct Q_p model. The Q values are clipped to 1,000 for a convenient display of the gas layer. The Q values are different in each layer and are larger than 1,000 in the nongas sand. [**ER**]

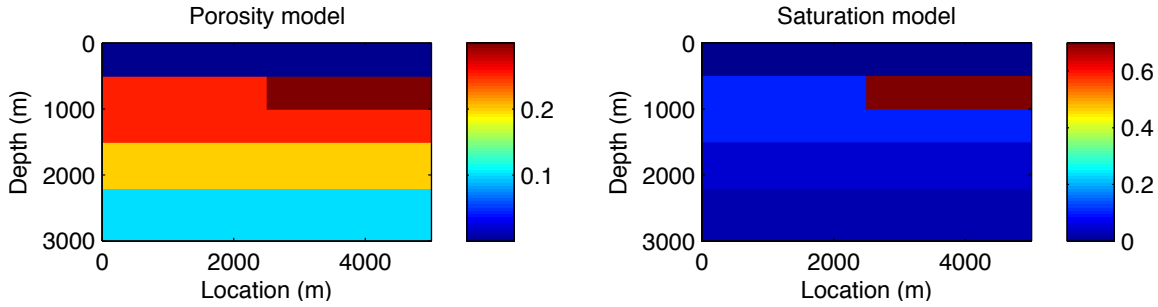

Figure 8: Rock properties: (a) porosity model; (b) gas saturation model. [**NR**]

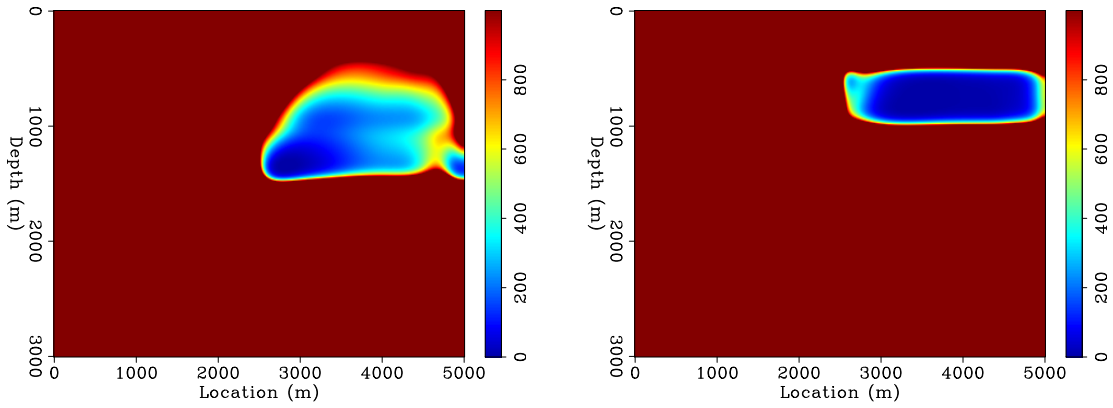

(a) (b)

Figure 9: (a) Inverted Q_p model without constraint. (b) Inverted Q_p model with constraint, with the parameters of gas sand:$c1 = 0.0038, c2 = 0.0029, c3 = 2.051{*}10^{-5}$ and non gas sand: $c1 = 0.0038, c2 = 0.0036, c3 = 5.97 * 10^{-6}$. [**ER**]

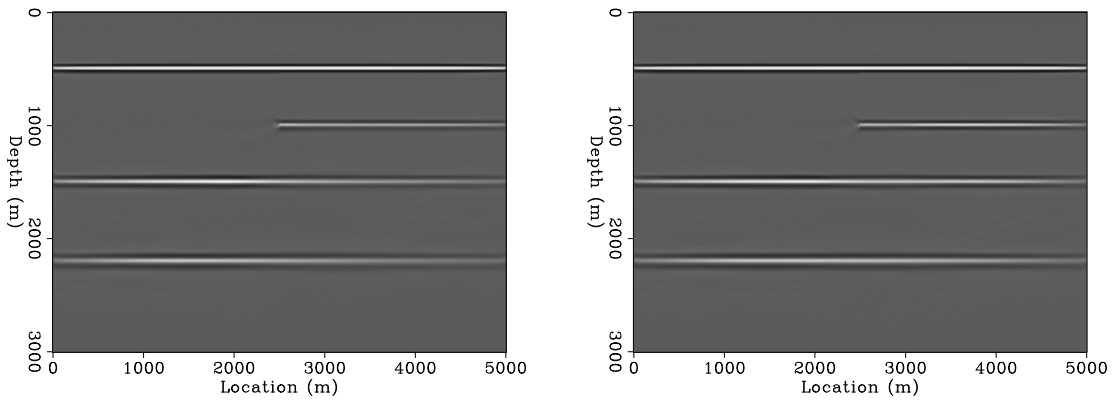

Figure 10: Prestack migration image: (a) Attenuated image; (b) Compensated image. [**ER**]

our new $Q_p - V_p$ equation to synthetic seismic data, which produced an improved Q estimated model. We showed that this improved Q model leads to a better seismic migration image.

REFERENCES

Billette, F. and S. Brandsberg-Dahl, 2005, The 2004 BP velocity benchmark: 67th Conference and Exhibition, EAGE, Extended Abstracts, B035.

Dvorkin, J., M. A. Gutierrez, and D. Grana, April 2014, Seismic reflections of rock properties: Cambridge University Press.

Dvorkin, J. and A. Nur, 1996, Elasticity of highporosity sandstones: Theory for two North Sea data sets: Geophysics, **61**, 1363–1370.

Gassmann, F., 1951, Uber die elastizitat poroser medien: Vierteljahrsschrift der Naturforschenden Gesellschaft in Zrich, **96**, 1–23.

He, Y. and J. Cai, 2012, Q tomography towards true amplitude image and improve sub-karst image: **521**, 1–5.

Li, Y., Y. Shen, and P. Kang, 2015, Integration of seismic and fluid-flow data: a two-way road linked by rock physics: EAGE – 77th EAGE Conference and Exhibition.

Mavko, G., T. Mukerji, and J. Dvorkin, 1991, The handbook of rock physics: Cambridge University Press.

Muller, T. M., B. Gurevich, and M. Lebedev, 2010, Seismic wave attenuation and dispersion resulting from wave-induced flow in porous rocks A review: Geophysics, **75**, A147–A164.

Raymer, L. L., E. R. Hunt, and J. S. Gardner, 1980, An improved sonic transit time-to-porosity transform: Society of Petrophysicists and Well-Log Analysts, **January**, no. 1.

Shen, Y., B. Biondi, R. Clapp, and D. Nichols, 2013, Wave-equation migration Q analysis (WEMQA): EAGE Workshop on Seismic Attenuation Extended Abstract.

———, 2014, Wave-equation migration Q analysis (WEMQA): SEG Technical Program Expanded Abstracts.

Wang, Y., S. Chen, L. Wang, and X. Li, 2013, Modeling and analysis of seismic wave dispersion based on the rock physics model: J. Geophys. Eng., **10**.

Zhou, J., X. Wu, K. H. Teng, Y. Xie, F. Lefeuvre, I. Anstey, and L. Sirgue, 2014, FWI-guided Q tomography and Q-PSDM for imaging in the presence of complex gas clouds, a case study from offshore Malaysia: **136**, 536–540.